Density-Tuned Polyolefin Phase Equilibria. 1. Binary Solutions of Alternating Poly(ethylene–propylene) in Subcritical and Supercritical Propylene, 1-Butene, and 1-Hexene. Experiment and Flory–Patterson Model

Shean-jer Chen and Maciej Radosz*

Exxon Research and Engineering Company, Route 22 East, Annandale, New Jersey 08801

Received November 26, 1991; Revised Manuscript Received December 17, 1991

ABSTRACT: Temperature–pressure phase boundaries are measured for solutions of alternating poly(ethylene–propylene) fractions in propylene, 1-butene, and 1-hexene. These amorphous fractions have similar structures and very narrow molecular weight distributions but differ in average molecular weight, from 0.79K to 96.4K. The phase transitions, typically in the form of a cloud-point transition, are determined in a variable-volume, optical cell up to 200 °C and 550 bar. The phase transitions are found to be dependent on the difference in size (molecular weight) between polyolefin and solvent. When the difference is large enough, the LCST and UCST curves merge into one curve that we refer to as U–LCST. The LCST, UCST, and U-LCST curves are correlated with Flory–Patterson's corresponding states theory.

Introduction

Polymer solutions are known to demix, i.e., to form two-phase systems, upon either decreasing temperature or increasing temperature, or both. To a first approximation, the low-temperature demixing is driven by enthalpy-related molecular forces. The high-temperature demixing, in addition to enthalpy-related forces, such as hydrogen bonding, can be driven by the difference in thermal expansion, and hence density, between the solvent and polymer. This effect, often referred to as the free-volume effect, becomes dominant near and above the solvent critical point, where the solvent density starts decreasing rapidly with increasing temperature. As usual, the two corresponding phase boundary curves are labeled as UCST (upper critical solution temperature) and LCST (lower critical solution temperature).[1,2] Although UCST and LCST refer to the two corresponding *critical points*, we will use these two terms as labels for the whole phase boundary *curves*. This does not imply that these curves are the critical locus curves. These curves are usually measured as cloud-point curves at the solution bubble-point pressure (close to the solvent vapor pressure).

Much less is known about the effect of pressure on polymer solution demixing. A pressure–temperature constant-composition phase diagram for nonassociating systems, such as hydrocarbons, is shown in Figure 1. This phase diagram qualitatively represents previous phase behavior data, including those obtained for near-critical and supercritical polymer systems.[3-5] The LV curve in Figure 1 is the liquid–vapor equilibrium curve, which is close to the solvent vapor-pressure curve and is terminated at the solvent critical point (filled circle). The LV curve becomes LLV (liquid–liquid–vapor) at low and high temperatures, at points marked UCEP and LCEP, which are the upper and lower critical end points, respectively. These are the points where the UCST and LCST curves intersect the LV curve. This phase diagram is strictly valid only for amorphous polymers with no solid–liquid transitions (characteristic of polymers that are partially crystallizable).

For a typical amorphous system, we may have a pair of UCST and LCST curves and a LV curve. This means that, in the temperature–pressure coordinates, there is a one-phase region above the LV curve and above/between the UCST and LCST curves, two two-phase regions, below

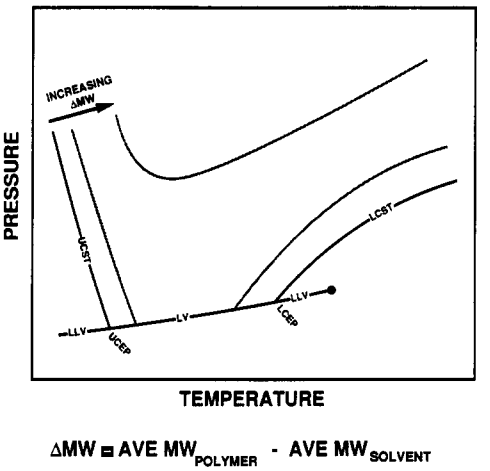

Figure 1. Pressure–temperature diagram for binary mixtures. LV, liquid + vapor; LLV, liquid 1 + liquid 2 + vapor; ΔMW, the molecular weight difference between two components. The heavy line represents the bubble-point pressure curve, which coincides with the solvent vapor-pressure curve in this study. The bold dot represents the critical point of the solvent.

(to the right of) LCST and below (to the left of) UCST, and two three-phase regions (LLV), below UCEP and above LCEP. The LLV region above LCEP extends up to about 3–5 °C above the solvent critical point.[6] As we increase the difference in size between the polymer and solvent, for example, by increasing the polymer molecular weight, we shift the LCST curve to lower temperatures and, simultaneously, we shift the UCST curve to higher temperatures. In other words, we cause these curves to approach each other and, eventually, merge into a single curve with a minimum,[5,7-9] as shown in Figure 1. We refer to this curve as a U–LCST curve because it has both UCST and LCST branches. Such a U–LCST curve corresponds to hourglass-shaped phase boundaries in temperature–composition phase diagrams.

The earliest interest in high-pressure phase behavior of polyolefin solutions can be traced to the development of polyethylene technology. The mutual miscibility of polyethylene and ethylene, in the form of cloud points, was measured by Ehrlich[10] and others.[11,12] The cloud-point data for other polyolefin systems were also reported.[4,5,7-9,13-16] In most cases,[5,7,8,10-14] commercial polymers having broad molecular weight distributions, and non-

0024-9297/92/2225-3089$03.00/0

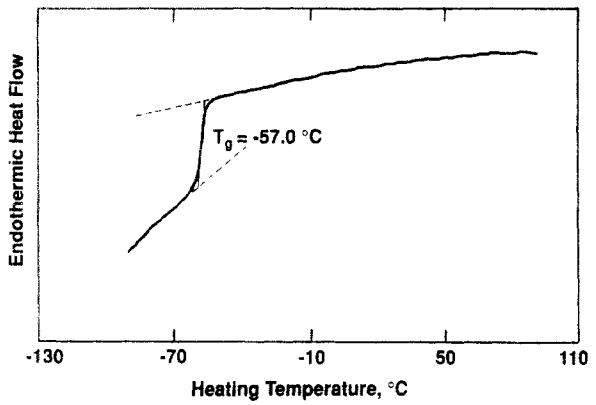

Figure 2. DSC thermogram for PEP96K, obtained at a heating rate of 10 °C/min. A single glass transition temperature (T_g = -57 °C), but no melting temperature, is found.

Table I
Molecular Weights and Characteristic Parameters for Poly(ethylene–propylene) Samples

sample code	M_w	M_w/M_n	T^*, K	P^*, bar	v^*, cm^3/g
PEP790	790	1.01	6562	4653	0.9927
PEP5.9K	5 900	1.08	6911	4719	0.9903
PEP26K	26 000	1.03	6895	4557	1.0005
PEP96K	96 400	<1.1	6903	4492	1.0021

uniform or unknown structure distribution, were used. While very useful in understanding basic phase diagram features, such data make it difficult to quantify, separate, and predict the effects of the average molecular weight, polydispersity, and structure. Therefore, our goal in this paper is to present phase boundaries of essentially monodisperse polyolefins with a well-defined and uniform structure in solutions with pure subcritical and supercritical olefins. In addition, we present a correlation of these data with a corresponding states theory developed by Flory[17] and Patterson.[18]

Experimental Section

Materials. The alternating poly(ethylene–propylene) samples used in this work are prepared by quantitative hydrogenation of polyisoprene synthesized through anionic polymerization with controlled 1,4-addition.[19] We refer to the hydrogenated samples as PEP790, PEP5.9K, PEP26K, and PEP96K, where the numbers correspond to the weight-average molecular weights. The polyisoprenes for PEP790 and PEP5.9K (CDS-I-9 and CDS-I-7, respectively) were purchased from Goodyear Tire & Rubber Co. (Akron, OH) and subsequently hydrogenated by L. J. Fetters. The polyisoprenes for PEP26K and PEP96K were synthesized and hydrogenated by L. J. Fetters, as shown.

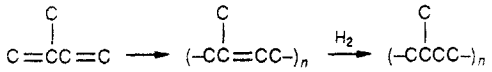

The polymers prepared by L. J. Fetters have a narrow molecular weight distribution and uniform structure. The sample codes, the weight-average molecular weights (M_w) from light scattering, and the polydispersity indices (weight-average to number-average molecular weight ratios, M_w/M_n) from size exclusion chromatography (SEC) are given in Table I. All the PEP samples are 100% amorphous, with a single glass transition. An example of a differential scanning calorimetry (DSC) trace is shown in Figure 2 for PEP96K.

Propylene (C.P. grade, 99.0% minimum purity) and 1-butene (C.P. grade, 99.0% minimum purity) were purchased from Matheson Gas Products, Inc. 1-Hexene (99.0% minimum purity) was purchased from Eastman Kodak Co. The physical properties of these materials are given in Table II.

Apparatus. The experimental apparatus and procedure used in this study are described in detail elsewhere.[20] Phase boundaries are measured in a batch optical cell equipped with a sapphire window and a movable piston, as shown in Figure 3. The piston controls volume, and hence pressure, at constant composition and temperature. The maximum volume is about 17 cm^3. Phase transitions are observed visually, typically in the form of cloud-point transitions, by displaying the window image, via borescope (Instrument Technology Series 123000) and a video camera, on a video screen (not shown in Figure 3). The cell, which is made of stainless steel 304 and sealed with two O-rings, is hydrotested up to 1200 bar at ambient temperature and used up to 550 bar at 200 °C. The cell is installed in an oven (Bemco Inc.) that can be controlled within 0.1 °C. The pressure is measured with a pressure transducer (Heise Model 623) with an accuracy of 0.3 bar. The pressure readings are checked against a dial gauge (Heise Model CM), which in turn is calibrated against a dead-weight tester (Ruska Corp.). The cell is equipped with three sampling lines and a mass spectrometer (UTI Instrument Model 100C) for analyzing gas compositions.

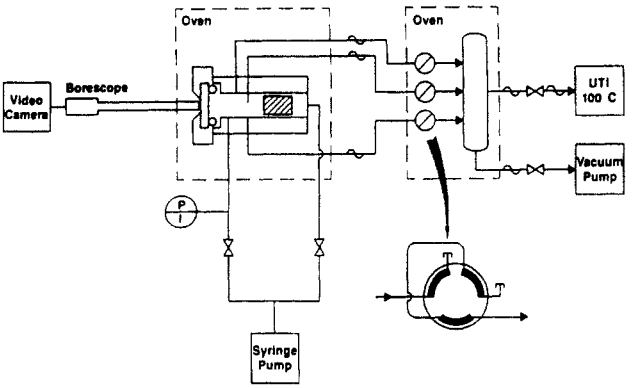

Figure 3. Simplified scheme of a MS batch cell. P, pressure transducer (Heise Model 623); UTI 100C, mass analyzer (UTI Instrument Model 100C).

Table II
Critical Constants and Characteristic Parameters for Solvents

solvent	T_c, K	P_c, bar	T^*, K	P^*, bar	v^*, cm^3/g
propylene	364.9	46.13	3329	3697	1.2478
1-butene	419.5	40.20	3875	3881	1.2162
1-hexene	503.9	31.40	4566	4096	1.1203

Procedure. The known amounts of polymer (from weighing) and solvent (from reading a syringe pump decal) are loaded into the cell. After allowing sufficient time for polymer swelling, up to 2 days depending on the polymer molecular weight and solvent, the solution is brought into the one-phase region by increasing the pressure while stirring. Next, the pressure is lowered slowly, while still stirring, until the mixture starts becoming cloudy. This indicates formation of a second phase. The corresponding pressure is recorded as the cloud-point pressure. In this study, we keep the polymer weight percent constant, about 15 wt %, which corresponds to typical commercial conditions. The exact composition of each solution is given in Table III.

The mixture compositions are obtained either from the known initial amount of each component (synthetic method) or from gravimetric–volumetric sampling (analytic method). The gravimetric–volumetric sampling method is illustrated in Figure 4. The one-phase polymer solution is sampled through a chromatographic valve (Valco UW Series) into a glassware trap filled with glass wool. The polymer is collected in the trap while the solvent vapor is collected in a graduated volumetric flask. The composition of the polymer solution in weight percent is calculated from the weights of the two components. Since 1-hexene is less volatile than the other solvents used, the compositions of 1-hexene solutions are determined by the synthetic method only. The compositions of polymer solutions in propylene, and in 1-butene, are determined by the analytic method. After measurements, the polymer left in the cell is dissolved in *n*-hexane and analyzed by SEC for traces of thermal degradation. No thermal degradation was found throughout all the experiments.

In addition to one-to-two and two-to-three phase boundaries, we observe two different patterns of phase disengagment which

Table III
LCEP,[a] $(dP/dT)_{LCEP}$, and Correlation Constants a and ν^2

solvent	polymer MW	polymer, wt %	LCEP, K	LCEP/T_c, K/K	$(dP/dT)_{LCEP}$, bar/deg	a	ν^2
propylene	790	17.2	351.1	0.962	1.75	0.500	0.0
	5 900	15.5	272.6	0.747	2.25	0.500	0.0110
	26 000	15.1				0.500	0.0264
	96 400	15.8				0.500	0.0247
1-butene	790	15.1					
	5 900	15.7	373.1	0.889	2.00	0.553	0.0
	26 000	16.0	345.1	0.822	2.00	0.512	0.0
	96 400	15.2	333.1	0.794	2.10	0.500	0.0
1-hexene	26 000	16.0	472.1	0.937	1.82	0.623	0.0
	96 400	15.0	457.1	0.907	1.79	0.547	0.0

[a] LCEP was obtained from the extrapolation of the LCST curve to the solvent vapor-pressure curve.

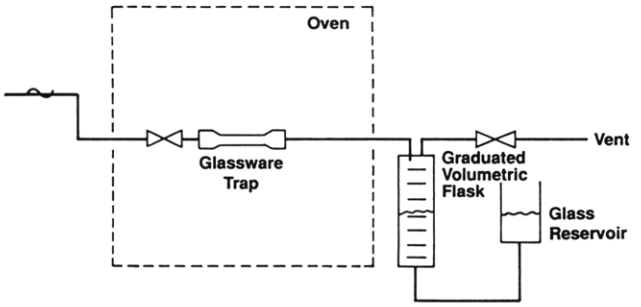

Figure 4. Schematic diagram of the sampling section. The valve (Valco UW Series) can be reached outside the oven.

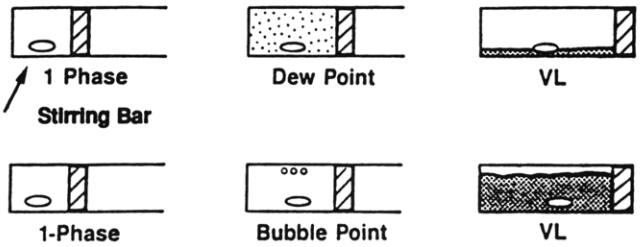

Figure 5. Schematic diagram of phase disengagement patterns. The shaded area represents a heavy (polymer-rich) phase.

are shown in Figure 5. One pattern is similar to a dew-point boundary in vapor–liquid equilibria, where one observes the onset and growth of the high-density phase (liquid) upon lowering pressure. Another pattern is similar to a bubble-point boundary in vapor–liquid equilibria, where one observes the onset and growth of the low-density phase (vapor) upon lowering pressure.

Results and Discussion

The data obtained in this work are given in Tables IV–VI. Solvent and polyolefin size effects on the phase behavior are discussed below.

Solvent Size Effect. We observe two basic types[6] of pressure–temperature phase diagrams for amorphous polymer–solvent systems: type A with a continuous critical locus connecting the solvent and polymer critical points and no LL split, and type B with UCST and LCST (or U–LCST) type critical loci. Type A is observed for polymers and solvents that do not differ much in size, while type B is observed for polymers and solvents that differ much in size. An example of these two types of phase diagrams is shown in Figure 6: PEP790 and 1-butene exhibit a type A phase behavior, while PEP790 and propylene exhibit a type B phase behavior. The LCEP point for propylene is around 78 °C. As in the following figures, open data points denote a dew-point-like phase boundary, whereas filled data points denote a bubble-point-like phase boundary. These boundaries divide the temperature–pressure surface into two regions for each system separately: one phase above and two phases below the boundary. Also, triangle points are used to indicate a two-to-three phase boundary, e.g., liquid–liquid to vapor–liquid–liquid in Figure 6 for propylene and PEP790. It turns out that the bubble-point pressure curve and the three-phase boundary are very close to the solvent vapor-pressure curve.

Table IV
Experimental Data for PEPs in Propylene

	T, °C (K)	P, bar	type of phase transition[a]
PEP790	46.3 (319.4)	19.0	VL(BP)
	70.2 (343.3)	30.2	VL(BP)
	77.4 (350.5)	34.4	VL(BP)
	79.0 (352.1)	37.7	LL(DP)
	81.9 (355.0)	43.0	LL(DP)
	100.2 (373.3)	73.0	LL(DP)
	124.8 (397.9)	113.0	LL(DP)
	150.0 (423.1)	144.0	LL(DP)
	174.8 (447.9)	170.0	LL(DP)
	200.2 (473.3)	190.0	LL(DP)
	79.0 (352.1)	35.9	VLL
	80.6 (353.7)	36.9	VLL
	81.9 (355.0)	38.3	VLL
PEP5.9K	−0.5 (272.6)	5.5	LL(DP)
	25.0 (298.1)	64.0	LL(DP)
	52.0 (325.1)	126.0	LL(DP)
	83.0 (356.1)	190.5	LL(DP)
	100.0 (373.1)	224.4	LL(DP)
	125.8 (398.9)	267.0	LL(DP)
	150.2 (423.3)	296.0	LL(DP)
	174.8 (447.9)	325.0	LL(DP)
	199.6 (472.7)	344.0	LL(DP)
PEP26K	50.4 (323.5)	273.0	LL(BP)
	82.4 (355.5)	312.0	LL(BP)
	100.2 (373.3)	332.0	LL(BP)
	124.9 (398.0)	361.2	LL(BP)
	150.4 (423.5)	388.0	LL(BP)
	175.0 (448.1)	412.0	LL(BP)
PEP96K	−9.0 (264.1)	354.0	LL(BP)
	−7.3 (265.8)	347.0	LL(BP)
	−2.0 (271.1)	337.0	LL(BP)
	1.0 (274.1)	331.0	LL(BP)
	4.8 (277.9)	325.5	LL(BP)
	7.2 (280.3)	322.5	LL(BP)
	12.1 (285.2)	316.7	LL(BP)
	13.9 (287.0)	315.0	LL(BP)
	20.4 (293.5)	311.0	LL(BP)
	29.9 (303.0)	310.6	LL(BP)
	44.0 (317.1)	319.5	LL(BP)
	49.4 (322.5)	322.3	LL(BP)
	60.0 (333.1)	330.0	LL(BP)
	81.5 (354.6)	352.0	LL(BP)
	99.9 (373.0)	371.0	LL(BP)
	124.6 (397.7)	396.4	LL(BP)
	150.2 (423.3)	423.0	LL(BP)
	174.8 (447.9)	442.3	LL(BP)
	200.4 (473.5)	461.0	LL(BP)

[a] VL, liquid–vapor equilibrium; LL, liquid–liquid equilibrium; VLL, vapor–liquid–liquid equilibrium; BP, bubble-point-like boundary; DP, dew-point-like boundary. PEP790, PEP5.9K, PEP26K, and PEP96K are characterized in Table I.

Table V
Experimental Data for PEPs in 1-Butene

	T, °C (K)	P, bar	type of phase transition[a]
PEP790	81.9 (355.0)	11.5	VL(BP)
	100.0 (373.1)	16.4	VL(BP)
	125.0 (398.1)	27.1	VL(BP)
	148.5 (421.6)	39.8	VL(BP)
	150.9 (424.0)	42.5	VL(BP)
	153.2 (426.3)	44.8	VL(DP)
	155.0 (428.1)	46.5	VL(DP)
	159.8 (432.9)	51.7	VL(DP)
	171.3 (444.4)	63.4	VL(DP)
	200.0 (473.1)	90.8	VL(DP)
PEP5.9K	103.0 (376.1)	21.3	LL(DP)
	105.7 (378.8)	27.2	LL(DP)
	109.5 (382.6)	35.3	LL(DP)
	124.8 (397.9)	66.7	LL(DP)
	150.0 (423.1)	110.0	LL(DP)
	174.8 (447.9)	146.0	LL(DP)
	200.0 (473.1)	172.5	LL(DP)
PEP26K	73.2 (346.3)	12.3	LL(BP)
	75.2 (348.3)	15.2	LL(BP)
	77.2 (350.3)	20.5	LL(BP)
	82.0 (355.1)	29.0	LL(BP)
	88.2 (361.3)	40.2	LL(BP)
	88.7 (361.8)	38.2	LL(BP)
	94.3 (367.4)	50.3	LL(BP)
	100.0 (373.1)	61.2	LL(BP)
	125.0 (398.1)	108.0	LL(BP)
	143.2 (416.3)	137.3	LL(BP)
	150.0 (423.1)	149.0	LL(BP)
	175.2 (448.3)	183.0	LL(BP)
	200.2 (473.3)	213.4	LL(BP)
PEP96K	61.3 (334.4)	8.4	LL(BP)
	62.9 (336.0)	13.1	LL(BP)
	66.4 (339.5)	19.5	LL(BP)
	70.6 (343.7)	28.4	LL(BP)
	82.0 (355.1)	54.0	LL(BP)
	100.0 (373.1)	90.8	LL(BP)
	125.0 (398.1)	137.3	LL(BP)
	150.6 (423.7)	177.3	LL(BP)
	175.0 (448.1)	210.1	LL(BP)
	200.0 (473.1)	240.5	LL(BP)

[a] VL, liquid–vapor equilibrium; LL, liquid–liquid equilibrium; VLL, vapor–liquid–liquid equilibrium; BP, bubble-point-like boundary; DP, dew-point-like boundary. PEP790, PEP5.9K, PEP26K, and PEP96K are characterized in Table I.

Table VI
Experimental Data for PEPs in 1-Hexene

	T, °C (K)	P, bar	type of phase transition[a]
PEP26K	174.8 (447.9)	12.7	VL(BP)
	194.7 (467.8)	17.2	VL(BP)
	200.0 (473.1)	23.5	LL(BP)
	204.8 (477.9)	29.4	LL(BP)
	205.5 (478.6)	31.6	LL(BP)
	200.0 (473.1)	19.3	VLL
	204.8 (477.9)	20.0	VLL
	205.4 (478.5)	20.4	VLL
PEP96K	143.8 (416.9)	8.3	VL(BP)
	180.0 (453.1)	14.0	VL(BP)
	186.2 (459.3)	18.3	LL(BP)
	191.8 (464.9)	28.5	LL(BP)
	201.3 (474.4)	43.3	LL(BP)
	190.8 (463.9)	17.3	VLL

[a] VL, liquid–vapor equilibrium; LL, liquid–liquid equilibrium; VLL, vapor–liquid–liquid equilibrium; BP, bubble-point-like boundary; DP, dew-point-like boundary. PEP790, PEP5.9K, PEP26K, and PEP96K are characterized in Table I.

The mixture critical temperatures are the points joining the bubble- and dew-point boundaries. An attempt to measure the critical temperatures on this basis, as suggested by de Loos,[11] is illustrated in Figure 7 for 1-butene and PEP790. Here, a relative cell height in percent is plotted as a function of pressure drop below the cloud-point pressure. In the dew-point experiments, we see an onset of the high-density phase and, upon coalescence and accumulation of this phase, a gradual rise of the interface,

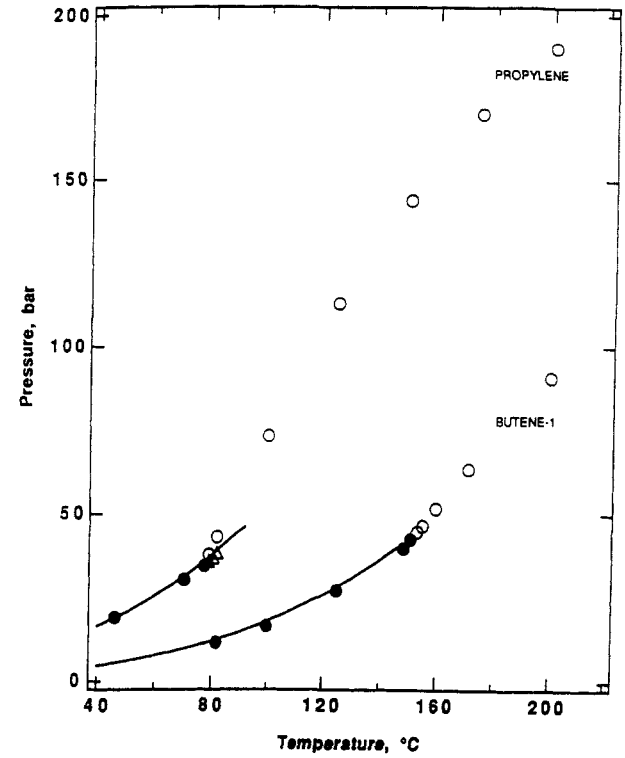

Figure 6. Pressure–temperature cloud-point curves for PEP790 in propylene (W_2 = 17.2 wt %) and in 1-butene (W_2 = 15.1 wt %). Open circles indicate a dew-point-like phase boundary while filled circles indicate a bubble-point-like phase boundary and triangles indicate a two-to-three phase boundary. The heavy lines are the vapor-pressure curves of the solvents.

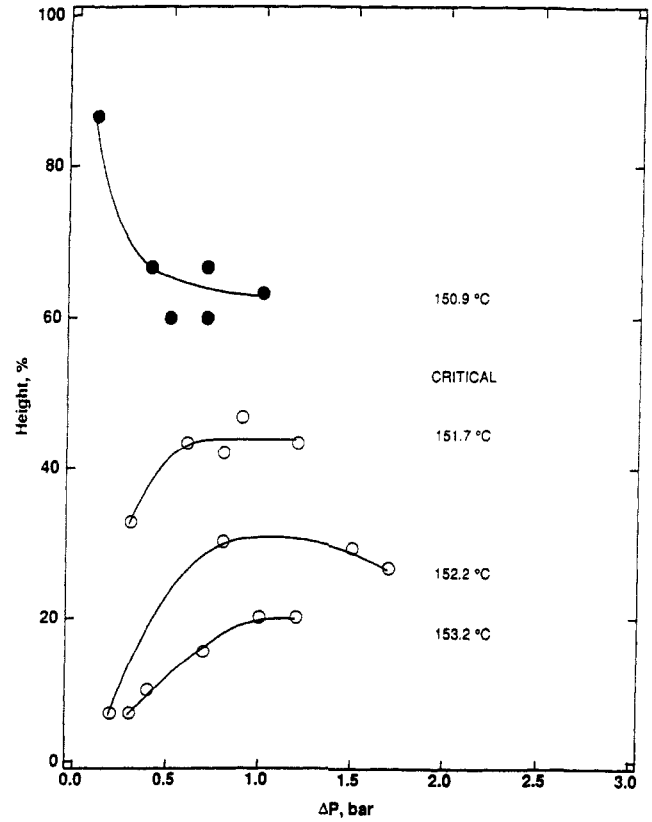

Figure 7. Plot of the relative cell height that the polymer-rich phase occupies as a function of the pressure drop, below the cloud-point pressure, for PEP790 in 1-butene (W_2 = 15.1 wt %).

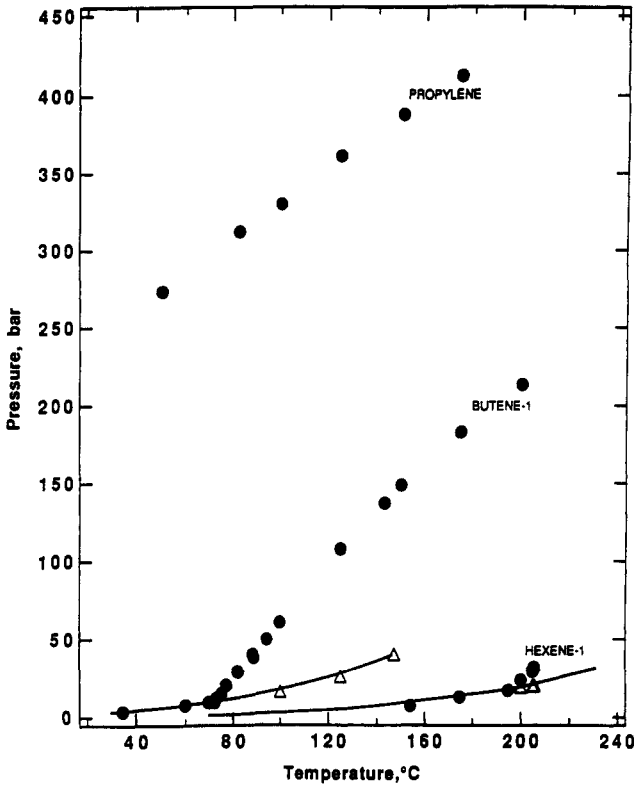

Figure 8. Pressure–temperature cloud-point curves for PEP26K in propylene (W_2 = 15.1 wt %), in 1-butene (W_2 = 16.0 wt %), and in 1-hexene (W_2 = 15.0 wt %). Open circles indicate a dew-point-like phase boundary while filled circles indicate a bubble-point-like phase boundary and triangles indicate a two-to-three phase boundary. The heavy lines are the vapor-pressure curves of the solvents.

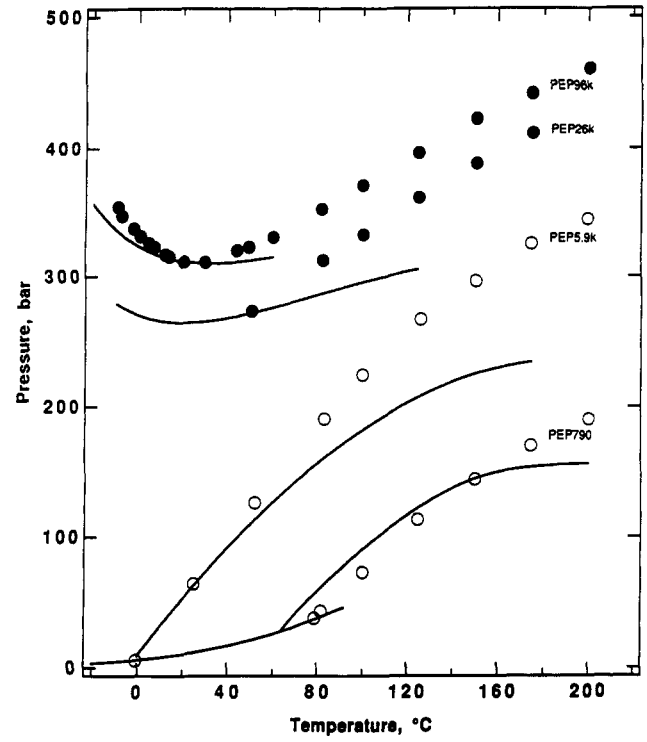

Figure 9. Pressure–temperature cloud-point curves for PEPs in propylene. From top to bottom, PEP96K (W_2 = 15.8 wt %), PEP26K (W_2 = 15.1 wt %), PEP5.9K (W_2 = 15.5 wt %), and PEP790 (W_2 = 17.2 wt %). Filled circles indicate a bubble-point-like phase boundary, and open circles indicate a dew-point-like phase boundary. The solid curves are calculated from eqs 2–8 with a = 0.500 for all polymers, and ν^2 = 0.0247, 0.0264, 0.011, and 0 for PEP96K, PEP26K, PEP5.9K, and PEP790, respectively.

from the bottom of the cell toward the middle (see Figure 5). By contrast, in the bubble-point experiments, we see an onset of the low-density phase (e.g., the first vapor bubble at the top of the cell) and a gradual drop of the interface, from the top of the cell toward the middle. As one iterates, by decreasing the dew-point temperature and increasing the bubble-point temperature, one converges around the critical temperature. In the example shown in Figure 7, the critical temperature lies between 150.9 and 151.7 °C, at 151.4 ± 0.2 °C.

The solvent effect for a higher molecular weight polymer (PEP26K) is shown in Figure 8. As a result of a greater degree of molecular asymmetry upon going from 1-hexene to propylene, we observe a shift of the LCST curves to higher pressures and lower temperatures. In other words, we increase the two-phase region. A small three-phase region found for 1-hexene is shown in the same figure. However, 1-hexene boundaries are at low pressures, not exceeding much the 1-hexene vapor pressures in the temperature range studied. LCEP for 1-hexene is estimated to be 199 °C. For 1-butene, LCEP is around 72 °C, and UCEP is around 147 °C, which is 1 °C above the 1-butene critical temperature.

In general, the smaller (hence weaker) the solvent, the higher the LCST pressure that is needed to keep the polymer in solution.

Polyolefin Size Effect. Polyolefin size is found to affect the phase boundaries in two important ways. Upon increasing the polyolefin size for a given solvent, one not only monotonically increases the LCST pressures but also observes a qualitative change in the phase disengagement patterns. This is illustrated in Figure 9 for propylene.

Upon going from PEP790 to PEP96K, we increase the LCST pressures by as much as 300 bar, for example, from about 100 to 400 bar at 120 °C and from about 200 to almost 500 bar above 200 °C. It is worth noting that the PEP790 and PEP5.9K boundaries are of the dew-point type, whereas the PEP26K and PEP96K boundaries are of the bubble-point type. This suggests a qualitative change in the phase disengagement patterns upon going from the molecular weight of 5.9K to 26K. Smaller polyolefins undergo a dew-point phase separation (polymer-rich phase precipitates from the solution first), while larger polyolefins undergo a bubble-point phase separation (solvent-rich phase separates out from the solution first). This also implies that the polymer concentration used in this work (about 15 wt %) is below the critical concentration for PEP790 and PEP5.9K but above the critical concentration for PEP26K and PEP96K[21] and that 15 wt % is the critical concentration in propylene for a PEP with a molecular weight between 5900 and 26 000.

The LCEPs for PEP790 and PEP5.9K in Figure 9 are +78 and −0.5 °C, respectively. The initial slopes, dP/dT at LCEP, of these two polymers in propylene are 1.75 and 2.25 bar/deg (see Table III), respectively. As the LCEP decreases, the value of dP/dT in a polymer–solvent system tends to increase.[22]

In an effort to find the UCEP for these two solutions upon cooling, in a glass tube experiment, PEP790 and PEP5.9K are mixed with propylene and sealed under vacuum when the solutions are frozen by liquid nitrogen. The solutions are found clear at temperatures down to −70 °C, which means that the UCEPs for these two solutions, if measurable, are below −70 °C.

In a similar glass tube experiment, 15 wt % mixtures of PEP26K and propylene, and PEP96K and propylene, remain cloudy from −70 to +50 °C along the propylene vapor-pressure curve. This means that PEP26K and PEP96 exhibit a U-LCST boundary. Such a U-LCST

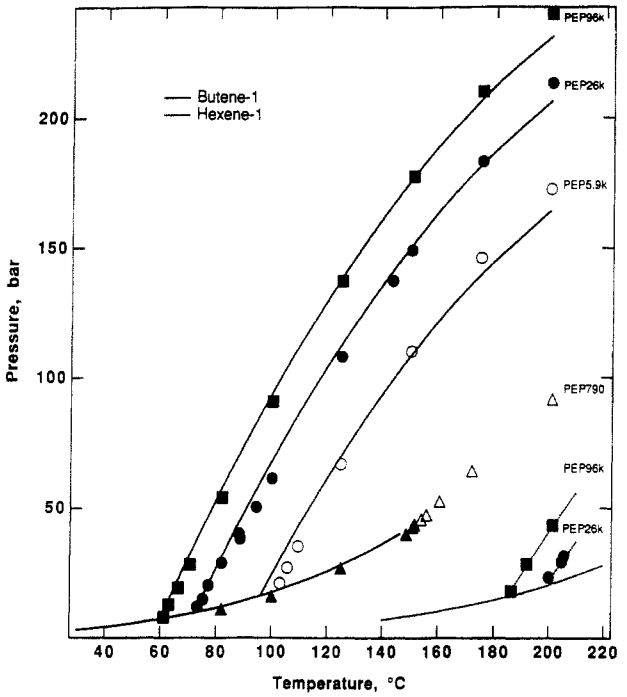

Figure 10. Pressure–temperature cloud-point curves for PEPs in 1-butene and in 1-hexene: squares, PEP96K; filled circles, PEP26K; open circles, PEP5.9K; triangles, PEP790. The concentrations are given in Table III. The curves are calculated from eqs 2–8 with $\nu^2 = 0$ and a given in Table III.

boundary is illustrated in Figure 9 for PEP96K and propylene. This boundary has a minimum between 22 and 30 °C. We note that the UCST branch of the U–LCST curve is not due to solid–liquid transition, which was observed for propane–polyethylene[23] and propane–poly(ethylene-*co*-methyl acrylate),[24] because PEP96K is 100% amorphous as shown in Figure 2.

This U–LCST type of behavior is in contrast to 1-butene and 1-hexene solutions shown in Figure 10. In both cases, no U–LCST curve is observed because the LCST boundaries are shifted to lower pressures relative to propylene. In other words, it takes much lower pressures to achieve a one-phase solution with 1-butene or 1-hexene than it does with propylene. Similar to propylene, the LCST pressures systematically increase upon increasing molecular weight.

In general, the larger the polymer, the higher the LCST pressure needed to keep the polymer in solution (in one phase).

LCST Pressure Dependence. The initial slopes of the LCST curves at LCEP are about 2.0 bar/deg for 1-butene and 1.8 bar/deg for 1-hexene (Figure 10; Table III), which are similar to other systems.[16,22] The fact that the 1-hexene slope is smaller, compared to 1-butene, illustrates a more general trend,[16,22] which is also observed for PEPs in propylene. The more general trend is that the initial LCST slopes decrease upon increasing LCEP, by either reducing the polymer size or increasing the solvent size, or both.

A quantitative LCST pressure dependence, strictly valid at the critical point, but usually used[7,10,13] for LCST curves, is given by[24]

$$(\partial P/\partial T)_c^{-1} = (\partial^2 \Delta V_{mix}/\partial W_2^2)_c/(\partial^2 \Delta S_{mix}/\partial W_2^2)_c \quad (1)$$

where subscript c denotes the critical curve, W_2 is the polymer weight percent, ΔV_{mix} and ΔS_{mix} are the volume and entropy of mixing, respectively. Hereafter, the subscripts 1 and 2 denote the solvent and polymer, respectively. At LCST, ΔS_{mix} is negative but has a positive curvature; i.e., $(\partial^2 \Delta S_{mix}/\partial W_2^2)_c$ is positive. ΔV_{mix} has been observed[26,27] to be usually negative for polymer–solvent mixtures, corresponding to a positive curvature of ΔV_{mix}-(W_2); i.e., $(\partial^2 \Delta V_{mix}/\partial W_2^2)_c$ is positive. Since both the numerator and denominator in eq 1 are positive, $(\partial P/\partial T)_c$ is also positive[4,16,22] for the LCST curve. This means that LCST pressures always increase upon increasing temperature, which is consistent with the free-volume interpretation of the LCST demixing.[1,2,17,18]

To a first approximation, the LCST demixing is driven by a large difference in free volume between the solvent and polymer. The solvent free volume increases (solvent expands) much more rapidly than that of the polymer, upon increasing temperature isobarically. This leads to LCST demixing. Therefore, higher pressures are required to compensate for this effect, to keep the free-volume difference between the solvent and polymer sufficiently low for complete miscibility.

Equation 1 is also valid for UCST. In this case, however, the denominator in eq 1 is negative. For example, combinatorial ΔS_{mix} given by the Flory–Huggins theory is positive but has a negative curvature. As mentioned before, the numerator is usually positive, which corresponds to a negative value of ΔV_{mix}. However, ΔV_{mix} can also be positive,[27] especially at low temperatures. Therefore, while $(\partial P/\partial T)_c$ is usually negative[16,22,28] for UCST, as shown in Figure 1, it can sometimes be positive. In fact, it has been found experimentally that while LCST pressures always increase upon increasing temperature,[4,9,16,22,28] the UCST pressures may either decrease or increase upon increasing temperature,[9,22,28] corresponding to negative and positive values of ΔV_{mix}, respectively.

Correlation. Corresponding states theories[17,18] have been extensively used to correlate LCST data. These theories utilize a polymer–solvent interaction parameter χ that is concentration dependent. The first, concentration-independent term in the power-series expansion of χ in concentration, referred to as χ_1, can be expressed[18] in terms of the solvent (subscript 1) reduced variables $\tilde{T}_1$, $\tilde{P}_1$, and $\tilde{V}_1$:

$$\chi_1/c_1 = (1/\tilde{T}_1\tilde{V}_1)\nu^2 + \tilde{C}_{p,1}(\tau + \pi\tilde{\beta}_1\tilde{P}_1/\tilde{\alpha}_1\tilde{T}_1)^2/2 \quad (2)$$

The first (ν^2-related) term in eq 2 is the energy term (dominant in the UCST phase transitions), and the second ($\tilde{C}_{p,1}$) term in eq 2 is the free-volume term (dominant in the LCST phase transitions). $3c_1$ is the number of the external degrees of freedom of the solvent molecule. $\tilde{T}_1$, $\tilde{P}_1$, and $\tilde{V}_1$ are the reduced solvent temperature, pressure, and volume, that is, T/T_1^*, P/P_1^*, and V_1/V_1^*, respectively. The parameter ν^2, conventionally used as a fitting parameter, is related to the cohesive energy and size difference between the solvent molecule (1) and the polymer segment (2). The parameter τ is related to the difference between the thermal expansion coefficients of the solvent (1) and polymer (2) and is defined[18] in terms of the characteristic temperature (reduction parameter) T^* as

$$\tau = 1 - (T_1^*/T_2^*) \quad (3)$$

The parameter π is defined[18] in terms of the characteristic pressure P^* as

$$\pi = (P_1^*/P_2^*) - 1 \quad (4)$$

$\tilde{C}_{p,1}$ is the reduced configurational heat capacity of the solvent, and $\tilde{\alpha}_1$ and $\tilde{\beta}_1$ are the reduced thermal expansion coefficient and the isothermal compressibility of the solvent, respectively. In order to derive $\tilde{C}_{p,1}$, $\tilde{\alpha}_1$, and $\tilde{\beta}_1$,

one needs an equation of state. In this work, we use an equation of state proposed by Flory et al.:[17]

$$\tilde{P}\tilde{V}/\tilde{T} = \tilde{V}^{1/3}/(\tilde{V}^{1/3} - 1) - 1/(\tilde{V}\tilde{T}) \quad (5)$$

On the basis of eq 5, Flory et al.[17] derive an expression for $\tilde{\beta}_1\tilde{P}_1/\tilde{\alpha}_1\tilde{T}_1$ as follows:

$$\tilde{\beta}_1\tilde{P}_1/\tilde{\alpha}_1\tilde{T}_1 = \tilde{P}_1\tilde{V}_1^2/(\tilde{P}_1\tilde{V}_1^2 + 1) \quad (6)$$

Also on the basis of eq 5, Patterson et al.[18] derive an expression for $\tilde{C}_{p,1}$:

$$\tilde{C}_{p,1} = [(1 - (2/3)\tilde{V}_1^{-1/3}) - 2(1 - \tilde{V}_1^{-1/3})/(\tilde{P}_1\tilde{V}_1^2 + 1)]^{-1} \quad (7)$$

Finally, our phase equilibrium condition in terms of the polymer–solvent interaction parameter χ_1, at the critical point, is given[18] as

$$\chi_1(\text{crit}) = a(1 + r^{-1/2})^2 \quad (8)$$

where a is set equal to 0.5 at the critical point or treated as an adjustable parameter away from the critical point, and r is the ratio of the molar volume reduction parameters (V_2^*/V_1^*). Combining eqs 2, 5, and 8 provides a means to calculate the critical loci of polymer solutions. Although this approach is strictly valid at the critical point, it has also been used[5,8,9,14,22] away from the critical point because the pressure–composition curves are flat in the neighborhood of the critical composition.[10,13,15,21,28] In other words, we assume that in the state of phase equilibrium the χ_1 calculated from eq 8 is equal to that calculated from eq 2.

In order to adopt this approach, we have to know the characteristic (reduction) parameters for each species. In this work, the reduction parameters for polymers are obtained by fitting the pressure–volume–temperature data[29] of polymers with eq 5 in a temperature range of 25–230 °C and in a pressure range of 1–2000 bar. The polymer parameters are given in Table I. The reduction parameters for solvents are calculated from the densities, thermal expansion coefficients, and isothermal compressibilities at zero pressure, according to Flory's method.[17] The solvent parameters are given in Table II. The values of T^* and P^* for solvents differ from those of corresponding[18] alkanes by less than 3%, and the values of V^* differ by less than 10%. Values of the reduction parameters tend to be temperature-dependent. However, we ignore the temperature dependence and treat them as constants in this work.

In our calculations, the parameter c_1 is set equal to $P_1^*V_1^*/RT_1^*$ as proposed by Flory et al.,[17] a is set equal to 0.5, and ν^2 is treated as an adjustable parameter. At a given temperature, eqs 5 and 2, with the χ_1 value calculated from eq 8, are solved simultaneously for the solvent reduced pressure $\tilde{P}_1$. We adjust ν^2 to match the reduced experimental LCST pressures. We find that ν^2 determined in this way must be negative for PEPs in 1-butene and in 1-hexene, which is physically unrealistic. A similar result was also obtained by others.[5,7,9,22]

Therefore, according to a method proposed by Patterson,[9,12] we allow a in eq 8 to be treated as an additional adjustable parameter with a value equal to or greater than 0.5. This will account not only for deviations due to noncritical compositions but also for ignoring the noncombinatorial (nonrandomness) entropy of mixing in the derivation of eq 8. Directionally, both noncombinatorial entropy and increasing a increase χ_1.

In practice, we adjust the values of a and ν^2 to fit one experimental data point for each system. Then we use these values of a and ν^2 (listed in Table III) to calculate all the other experimental points. Incidentally, Saraf and Kiran[15] treat both c_1 and $c_1\nu^2$ as adjustable parameters in calculating the critical lines of polystyrenes in n-butane and in n-pentane, which is similar to our approach.

For 1-butene and 1-hexene, ν^2 is found to be equal to 0. This implies that the LCST pressure is primarily dependent on the free-volume term in eq 2 and independent of the energy term. It turns out that a is equal to 0.5 for PEP96K and 1-butene and increases with a decrease in the molecular weight of the polymer. As shown in Figure 10 the calculated curves are in good agreement with the experimental data for 1-butene and 1-hexene.

In addition to the values of ν^2 and a, Table III gives the absolute values of LCEP and the reduced values of LCEP/T_c, which characterize the location of LCEP relative to the solvent critical temperature. LCEP/T_c varies not only from polymer to polymer for a given solvent but also from solvent to solvent for a given polymer. LCEP/T_c is related to the parameter τ. This is because, for a constant χ_1 in eq 2, when τ is larger, $\tilde{C}_{p,1}$ has to be smaller, which implies that $\tilde{V}_1$ has to be smaller and hence $\tilde{T}_1$ has to be lower. In brief, this qualitative analysis of eq 2 suggests that when τ is large, e.g., for small solvents, LCST temperature ($\tilde{T}_1$; hence, LCEP/T_c) will be low. Conversely, when τ is small, e.g., for large solvents, LCST temperature ($\tilde{T}_1$; hence, LCEP/T_c) will be high.

Our results confirm these trends. The τ value for 1-butene is greater than that of 1-hexene, as can be estimated from T^* values given in Table II. Therefore, as expected, the LCEP/T_c values estimated based on the data from Table III for a given polymer are always greater for 1-hexene than 1-butene, as shown.

	1-butene	1-hexene
PEP96K	0.794	0.907
PEP26K	0.822	0.937

In contrast to the 1-butene and 1-hexene data discussed above, the propylene data cannot be reproduced with ν^2 set equal to zero. In fact, we find that ν^2 for propylene has to always be nonzero and positive for positive values of a. Since a has to be equal to or greater than 0.5, the propylene data are fitted by setting $a = 0.500$ and by adjusting ν^2 only. The fitting results are shown in Figure 9. The agreement with experimental data is not as good as that for 1-butene and in 1-hexene. For PEP790, the predicted curve deviates from the experimental data significantly at higher temperatures, and LCEP is about 16 °C lower than the experimental value. For PEP5.9K, the predicted curve is also off above 100 °C. The quality of fit is even worse for PEP26K and PEP96K, especially at higher temperatures. Therefore, for better clarity, we do not extend the predicted curves for PEP26K and PEP96K (Figure 9) to higher temperatures. Upon increasing temperature, these predicted curves deviate rapidly from the experimental data because their slope is wrong. By increasing a we can shift the calculated curves to lower pressures but cannot change the slopes of the curves and thus cannot improve the fit quality. The fit quality can be improved if one allows the characteristic reduction parameters to be temperature-dependent.[8] However, we do not choose this option. Instead, we use a different approach, utilizing an equation of state based on the statistical associating fluid theory, which is a subject of our next paper.[31]

The energy term in eq 2, which accounts for the contact energy dissimilarity, increases with decreasing temperature and thus should lead to UCST at low temperatures.

For PEPs in 1-butene and in 1-hexene, and PEP790 and PEP5.9K in propylene, the Flory–Patterson theory does not predict the existence of UCST because the ν^2 values are zero or close to zero. However, upon increasing ν^2, the Flory–Patterson model correctly predicts merging the UCST and LCST curves into a U–LCST curve for PEP26K and PEP96K in propylene. As shown in Figure 9, the theory predicts the U–LCST curve for both mixtures with a small ν^2 value.

The value of ν^2 is equivalent to a X_{12}/P_1^* term in the Flory[17] theory, where X_{12} is the interchange contact energy between unlike molecules. The ν^2 values obtained for PEPs in propylene correspond to X_{12} in a range of 0.97–2.33 cal/cm^3. Similar X_{12} values are reported[26,30] for other aliphatic–aliphatic pairs. In addition, for polyisobutene solutions in n-alkanes Flory et al.[26] find that the X_{12} values decrease with an increase in the alkane chain length and become close to zero in the limit of an infinite alkane chain. Our results are consistent with this trend.

Conclusion

Poly(ethylene–propylene) phase behavior in solutions with subcritical and supercritical olefins is related to differences in the polyolefin and solvent size. The greater the difference, (1) the higher the probability of type B phase behavior and (2) the higher the LCST pressure. The pressure effect on LCST can be captured by Flory and Patterson's corresponding states theory. This theory can also predict U–LCST curves, which are observed when UCST and LCST curves merge for large polymers and small solvents.

Acknowledgment. We are grateful to Lewis J. Fetters for sharing with us his poly(ethylene–propylene) samples. Special thanks are due to C. K. Chen for SEC analysis and D. T. Hseih for DSC measurements. Stimulating discussions with N. Baron, Y. C. Chiew, C. Cozewith, B. Folie, and J. L. Hemmer are also gratefully acknowledged. A preliminary account of this work was presented at the 2nd International Symposium on Supercritical Fluids, Boston, MA, 1991.

References and Notes

(1) Saeki, S.; Kuwahara, N.; Konno, S.; Kaneko, M. *Macromolecules* **1973**, *6*, 246, 589.
(2) Casassa, E. F.; Berry, G. C. In *Comprehensive Polymer Science*; Allen, G., Revington, J. C., Eds.; Pergamon: New York, 1988; Vol. 2, pp 100–110.
(3) McHugh, M. A.; Krukonis, V. J. *Supercritical Fluid Extraction*; Butterworth: Boston, MA, 1986; Chapter 9.
(4) Allen, G.; Baker, C. H. *Polymer* **1965**, *6*, 181.
(5) McClellan, A. K., Bauman, E. G., McHugh, M. A. In *Supercirtical Fluid Technology*; Penninger, J. M. L., Radosz, M., McHugh, M. A., Krukonis, V. J., Eds.; Elsevier: Amsterdam, The Netherlands, 1985; pp 161–178.
(6) Radosz, M. *Ind. Eng. Chem. Res.* **1987**, *26*, 2134.
(7) McHugh, M. A.; Guckes, T. L. *Macromolecules* **1985**, *18*, 674.
(8) Seckner, A. J.; McClellan, A. K.; McHugh, M. A. *AIChE J.* **1988**, *34*, 9.
(9) Zeman, L.; Patterson, D. *J. Phys. Chem.* **1972**, *76*, 1214.
(10) Ehrlich, P. *J. Polym. Sci.* **1965**, *A3*, 131.
(11) de Loos, T. W.; Poot, W.; Diepen, G. A. M. *Macromolecules* **1983**, *16*, 111.
(12) Spahl, R.; Luft, G. *Ber. Bunsen-Ges. Phys. Chem.* **1982**, *86*, 621.
(13) Ehrlich, P.; Kurpen, J. J. *J. Polym. Sci.* **1963**, *A1*, 3217.
(14) Iran, C. A.; Cozewith, C. *J. Appl. Polym. Sci.* **1986**, *31*, 1879.
(15) Saraf, V. P.; Kiran, E. *J. Supercrit. Fluids* **1988**, *1*, 37.
(16) Saeki, S.; Kuwahara, N.; Kaneko, M. *Macromolecules* **1976**, *9*, 101.
(17) Flory, P. J.; Orwoll, R. A.; Vrij, A. *J. Am. Chem. Soc.* **1964**, *86*, 3507, 3515.
(18) Patterson, D.; Delmas, G. *Trans. Faraday Soc.* **1969**, *61*, 708.
(19) Mays, J.; Hadjichristidis, N.; Fetters, L. J. *Macromolecules* **1984**, *17*, 2723 and references therein.
(20) Chen, S.-j.; Randelman, R.; Seldomridge, R. J.; Radosz, M. Presented at the Annual AIChE Meeting, Chicago, IL, Nov 1990; Paper 32a.
(21) Chen, S.-j.; Gregg, C. J.; Radosz, M., unpublished results.
(22) Zeman, L.; Biros, J.; Delmas, G.; Patterson, D. *J. Phys. Chem.* **1972**, *76*, 1206.
(23) Watkins, J. J.; Krukonis, V. J.; Condo, P. D., Jr.; Pradhan, D.; Ehrlich, P. *J. Supercrit. Fluids* **1991**, *4*, 24.
(24) Meilchen, M. A.; Hasch, B. M.; McHugh, M. A. *Macromolecules* **1991**, *24*, 4874.
(25) Rowlinson, J. S.; Swinton, F. L. *Liquids and Liquid Mixtures*, 3rd ed.; Butterworth: London, 1982; pp 115–119.
(26) Flory, P. J.; Ellenson, J. L.; Eichinger, B. E. *Macromolecules* **1968**, *1*, 279.
(27) (a) Eichinger, B. E.; Flory, P. J. *Trans. Faraday Soc.* **1968**, *64*, 2035, 2053, 2061, 2066. (b) Höcker, H.; Flory, P. J. *Trans. Faraday Soc.* **1971**, *67*, 2258, 2270. (c) Höcker, H.; Shih, H.; Flory, P. J. *Trans. Faraday Soc.* **1971**, *67*, 2275.
(28) Saeki, S.; Kuwahara, N.; Nakata, M.; Kaneko, M. *Polymer* **1975**, *16*, 445.
(29) Chiew, Y. C.; Chen, S.-j.; Gardecki, J.; Nilsen, S.; Radosz, M., unpublished results.
(30) Flory, P. J. *Discuss. Faraday Soc.* **1970**, *49*, 7.
(31) Chen, S.-j.; Economou, I.; Radosz, M., submitted for publication in *Macromolecules*.

Registry No. Propylene, 115-07-1; 1-butene, 106-98-9; 1-hexene, 592-41-6.